Title

Fourier Transform-Ion Cyclotron Resonance Mass Spectrometry as a Platform for Characterizing Multimeric Membrane Protein Complexes.

Journal

Journal of the American Society for Mass Spectrometry, 29(1)

Authors

Lippens, Jennifer
Nshanian, Michael
Spahr, Chris
et al.

Publication Date

2018

DOI

10.1007/s13361-017-1799-4

Peer reviewed

HHS Public Access

Author manuscript

J Am Soc Mass Spectrom. Author manuscript; available in PMC 2019 January 01.

Published in final edited form as:

J Am Soc Mass Spectrom. 2018 January ; 29(1): 183–193. doi:10.1007/s13361-017-1799-4.

Fourier Transform-Ion Cyclotron Resonance Mass Spectrometry as a Platform for Characterizing Multimeric Membrane Protein Complexes

Jennifer L. Lippens[1], **Michael Nshanian**[2], **Chris Spahr**[1], **Pascal F. Egea**[3], **Joseph A. Loo**[2,3,*], and **Iain D.G. Campuzano**[1,*]

[1]Discovery Analytical Sciences, Amgen, Thousand Oaks, California 91320, United States

[2]Department of Chemistry and Biochemistry, University of California-Los Angeles, Los Angeles, California 90095, United States

[3]Department of Biological Chemistry and Molecular Biology Institute, University of California-Los Angeles, Los Angeles, California 90095, United States

Abstract

Membrane protein characterization is consistently hampered by challenges with expression, purification and solubilization. Among several biophysical techniques employed for their characterization, native-mass spectrometry (MS) has emerged as a powerful tool for the analysis of membrane proteins and complexes. Here, two MS platforms, the FT-ICR and QToF, have been explored to analyze the homotetrameric water channel protein, AquaporinZ (AqpZ) under non-denaturing conditions. This 97 kDa membrane protein complex can be readily liberated from the octylglucoside (OG) detergent micelle under a range of instrument conditions on both MS platforms. Increasing the applied collision energy of the FT-ICR collision cell yielded varying degrees of tetramer (97 kDa) liberation from the OG micelles, as well as dissociation into the trimeric (72 kDa) and monomeric (24 kDa) substituents. Tandem-MS on the Q-ToF yielded higher intensity tetramer signal and, depending on the m/z region selected, the observed monomer signal varied in intensity. Precursor ion selection of an m/z range above the expected protein signal distribution, followed by mild collisional activation is able to efficiently liberate AqpZ with a high S/N ratio. The tetrameric charge state distribution obtained on both instruments demonstrated superpositioning of multiple proteoforms due to varying degrees of N-terminal formylation.

Introduction

Membrane proteins are responsible for many cellular processes, such as ion transport and molecular recognition [1, 2]. Currently, membrane proteins constitute at least 50% of prospective therapeutic targets [3, 4], making their structural characterization a high priority. Their structure and binding properties are vital pieces of required information for comprehending their capacity as potential therapeutic targets. Yet, in spite of high interest, membrane proteins represent less than 10% of the total solved structures in the Protein Data

*Correspondence to: Iain Campuzano; iainc@amgen.com, Joseph A. Loo; jloo@chem.ucla.edu.

Bank [4-7] and only 707 unique membrane protein structures are named in the Structural Biology Knowledgebase (http://blanco.biomol.uci.edu/mpstruc) [8]. The dearth of solved structures and complete characterization of these proteins comes as a direct consequence of their demanding nature when it comes to expression, purification and solubilization [9], which make them particularly challenging to investigate by traditional structural elucidation techniques such as nuclear magnetic resonance (NMR) and X-ray crystallography [10-14]. Over the past decade, native-mass spectrometry (native-MS) [9, 15] has proven to be a highly enabling and complementary biophysical technique for membrane protein characterization.

Native-MS provides a unique platform for rapid characterization with the benefit of low sample consumption, a particularly important attribute considering the poor expression of these proteins [9]. While monomeric membrane proteins, such as bacteriorhodopsin and bovine rhodopsin, have been investigated by native-MS [16], a vital turning point in the utilization of native-MS for membrane protein characterization came in 2008 with the observation of the intact heterotetrameric membrane and soluble protein complex, $BtuC_2D_2$ [17]. This analysis has been subsequently followed by numerous successful native-MS investigations of various membrane protein complexes, such as *Thermus thermophilius* V-type ATPase [18] and the trimeric OmpF porin [15, 19]. However, this native-MS strategy still requires the membrane protein to be solubilized, typically in a detergent micelle, which can in fact continue to encapsulate the protein even after introduction of the protein to the gas-phase. Therefore, mild collision induced dissociation (CID) is frequently employed to promote protein liberation from the detergent micelle and subsequent molecular weight (MW) determination [20]. Other activation/dissociation methods, such as infrared multiphoton dissociation (IRMPD), have also been demonstrated to efficiently liberate a membrane protein from a detergent micelle [21, 22]. Activation of the protein-detergent assembly through the application of collision energy (50 to 70 V) typically results in improved signal-to-noise (S/N) and high protein-to-detergent (P/D; Eq. 1) signal ratios.

$$\mathrm{P/D}=\frac{\text{Intensity of Protein Signal}}{\text{Intensity of Detergent Signal}} \quad \text{Eq. 1}$$

Yet, with the application of collision energy, it is critical to strike a balance between release of the membrane protein from the detergent micelle and dissociation of the intact membrane protein [20, 22, 23]. This is of particular importance for the analysis of membrane protein complexes, i.e., protein-protein and protein-ligand complexes, as preservation of these fragile interactions in the gas-phase while simultaneously disrupting the detergent micelle can be challenging. Therefore, in many cases, complete removal of detergent micelle signal from the spectrum may not be achieved. Besides detergents, there are other solubilzation methods currently under investigation for their ability to provide high quality MS data [24-26]. Some of these methods include nanodiscs (a phospholipid bilayer contained within two membrane scaffold proteins) [27, 28], styrene-maleic acid copolymers (SMA; polymers that self-insert into the membrane and extract regions of intact membrane containing membrane proteins and associated lipids) [29] and amphipols (amphipathic copolymers that

bind to the membrane protein) [25, 26]. Nevertheless, detergents remain the most common membrane mimetic by which membrane proteins are solubilized and analyzed by native-MS.

To date, reported native-MS membrane protein research has been heavily dominated by the use of quadrupole time-of-flight (Q-ToF) MS analyzers. Recently however, Orbital trapping instruments (Orbitrap) have become increasingly employed and are an attractive alternative to Q-ToF devices due to their apparent high resolving power and improvement in spectral quality without the need for extensive post data acquisition processing [22, 23, 30]. However, it should be noted that real time enhanced Fourier transformation (eFT) data processing occurs on these platforms [31, 32]. Given the variety of available MS instrumentation, it is important that the distinct advantages of individual MS platforms be highlighted and leveraged to provide comprehensive native-MS characterization. Here we present the characterization of a multimeric membrane protein complex, *Escherichia coli* AquaporinZ (AqpZ), a homotetramer (97 kDa) and highly efficient water channel protein, using a Fourier transform ion cyclotron resonance (FT-ICR) mass spectrometer. We aim to provide an unbiased comparison of the data quality between this platform and a typical Q-ToF platform regularly employed for membrane protein analysis, as well as highlight how each platform was leveraged for AqpZ characterization.

Experimental

Materials

The detergent *n*-octyl β -D-glucopyranoside (OG) used for solubilization was purchased from Anatrace (O311S; Maumee, OH). Gold-coated nano-ESI needles were purchased from Waters MS-Technologies (M956232AD1, long thin wall; Manchester, UK). Sulfur hexafluoride (SF_6) was purchased from Airgas (Palmdale, CA) and used as the collision gas in both the collision cell (FT-ICR) and Trap (Synapt G2). BioRad P6 spin columns used for buffer exchange were purchased from BioRad (732-6221, Hercules, CA). Trypsin was a product of Sigma-Aldrich (T-6567; St. Louis, MO). Chymotrypsin was purchased from Thermo Scientific (90056; Rockford, IL). Lys-C was a product from Wako (129-02541; Osaka, Japan). The preparation and purification of the AqpZ protein complex is detailed in the Supporting Information.

Native Mass Spectrometry Instrumentation and Sample Preparation

A 15-Tesla Solarix FT-ICR mass spectrometer (Bruker Daltonics; Bremen, Germany) and a Synapt G2 quadrupoleion mobility MS instrument (Waters MS-Technologies; Manchester, UK) were used to generate native-MS spectra. Specific acquisition collision voltages, source Skimmer 1 and collision cell voltages (FT-ICR) and sampling cone and trap voltages (Q-ToF), are explicitly discussed with the results obtained from those settings on each instrument. For other FT-ICR and Q-ToF instrument settings please refer to the Supporting Information. For all AqpZ experiments, sulfur hexafluoride (SF_6) was used as the collision gas in the collision cell (FT-ICR) and trap (Q-ToF). In general, 60 μM AqpZ stock was buffer exchanged after SEC purification (Supporting Information) using the BioRad P6 spin columns into 200 mM ammonium acetate with 1.1% (w/v) OG (two times the critical micelle concentration; 2× CMC). This stock solution was then diluted to 15-30 μM for

native-MS analysis, depending on the instrumentation used. Following buffer exchange, the AqpZ solution was loaded into a gold-coated borosilicate needle and analyzed in positive ion mode by nanoflow-ESI.

Denatured Protein Mass Spectrometry

LC-MS was performed with an Agilent 1200 series HPLC, using a ZORBAX 300SB-C3 (2.1×50 mm, 1.8 μM) column (857750-909, Agilent Technologies, Santa Clara, CA) in line with a Synapt G2 mass spectrometer (Waters MS-Technologies; Manchester, UK) during the 15 minute gradient. This 15 minute gradient employed 0.1% formic acid in H_2O as mobile phase A and 0.1% formic acid in acetonitrile as mobile phase B. The gradient was maintained at 5% B from 0-5 minutes, then increased to 95% B and held there from 5- 9 minutes. After this period, the gradient was brought back to 5% B for the remaining 6 minutes. The flow rate for the gradient was 0.250 mL/min and the column temperature was 40 °C. Zero-charge MW values for the AqpZ species were determined using MaxEnt 1 [33] in the MassLynx software (Waters MS-Technologies, UK). For deconvolution, the output mass range was set to 10,000:40,000 Da (chosen based on the expected mass of the monomeric species); 0.20 Da/channel resolution; minimum intensity ratio left and right at 50% width at half height for uniform Gaussian model at 0.750 Da with iterations to convergence.

LC-MS/MS of Proteolytically Digested AqpZ

Trypsin and chymotrypsin digestion conditions were as follows: 15 μg of AqpZ was combined with digestion buffer and urea to final concentrations of 37.5 mM Tris (pH 7.5), 2 M urea and 10 mM hydroxylamine. Lys-C digest conditions were as follows: 15 μg of AqpZ, however in final concentrations of 75 mM Tris (pH 7.5), 4 M urea and 20 mM hydroxylamine. Each digestion was brought to a total volume of 30 μL with deionized water after the addition of 1 μL of the respective enzyme to maintain an enzyme-to-substrate ratio (w/w) of 1:15. All digestions were incubated overnight at 37 °C, after which 30 μL of 0.1% formic acid was added, followed by 25 mM tris (2-carboxyethyl) phosphine (TCEP) for an incubation period of 15 minutes at 37 °C prior to LC-MS/MS analysis.

The proteolytic digests were measured by LC-MS/MS using a Waters NanoAcquity LC and LC-MS/MS interfaced to a Thermo OrbiTrap Velos MS (Thermo Scientific; Waltham, MA). The HPLC utilized a Symmetry C18 180 μm× 20 mm trapping column (Waters Corporation; part# 186006527) in-line and preceding a ZORBAX 300SB-C18 5 μm, 250× 0.5 mm analytical column (Agilent Technologies; part# 5064-8266). For peptide separations, mobile phases A and B consisted of 0.1% formic acid in H_2O and 0.1% formic acid in acetonitrile, respectively. Digests were loaded for 5 minutes onto the trap column using 3% B at a flow rate of 8 μL/min. Peptides were separated at 12 μl/min on the analytical column using the following gradient: 0 minutes at 3% B, up to 45% B over 85 minutes, up to 97% B over 1 minute, isocratic at 97% B for 6 minutes, down to 3% B over 3 minutes, and then isocratic at 3% B for 20 minutes. AqpZ digested with either trypsin, chymotrypsin or Lys-C was analyzed by LC-MS/MS using a full MS scan of *m/z* 300-2000 at 30k resolution (FWHM), followed by low resolution CID scans of the top 6 most abundant precursors. A spray

voltage of 4.5 kV, an S-Lens RF level of 50, an isolation width of 2.0 Da, a collision energy (CE) of 35 V and a 15 second dynamic exclusion were used.

Targeted CID and higher-energy collisional dissociation (HCD) experiments were performed on the singly charged ions (unmodified: 453.2224 Da and modified: 480.2182 Da) of the peptide ***MFR*** (amino acids 1-3 of the full length monomer) obtained from the tryptic digest. CID and HCD mass spectra were collected at 7.5k resolution using CE values of 35 V and 29 V respectively. Other instrumental parameters were kept consistent, as above (spray voltage, isolation width, etc.).

Results and Discussion

Regions of Collisional Activation for Detergent Micelle Disruption on the FT-ICR and Q-ToF Platforms

Historically, the process of membrane protein liberation from detergent micelles by native-MS is achieved by increasing the overall activation energy of the MS system (typically sample cone and collision cell) until the micelle is disrupted, and the protein is liberated [20]. This technique has been vastly employed for the analysis of many membrane proteins [20, 34, 35]. Each unique MS platform has various regions where voltage settings can be manipulated to provide the necessary energy to achieve protein liberation. The source region of the FT-ICR houses a 300 mm heated glass capillary that provides a long desolvation region, which introduces the protein ions to the high vacuum regions of the instrument from the ambient atmosphere. Following this capillary, there are two funnel stacks each followed by a skimmer, the voltage of which can be manipulated to aid in ion transmission as well as to generate various levels of in source dissociation. One of the two FT-ICR voltages investigated in this study, Skimmer 1 (Skim1), is located at the end of the funnel 1 stack (Figure 1a) and creates a voltage gradient such that if the voltage is high the ions will be accelerated into the funnel 2 stack -potentially producing in-source dissociation. The second voltage manipulated on this platform to achieve protein ejection was applied in the collision cell, which is located after the quadrupole and prior to the magnet. Application of collision energy and resultant ion-neutral collisions disrupt the detergent micelle to allow for protein ejection so that the membrane protein complex is ultimately detected. Increased application of this voltage can also generate dissociation of the protein into its constituent subunits (monomer and trimer).

Alternatively, the nanoflow-ESI source of the Synapt G2 quadrupole-ion mobility MS instrument does not utilize a heated capillary for ion transfer from ambient conditions to the vacuum regions of the instrument and instead utilizes dual orthogonal ion sampling (Z-spray) which can be held from 2-6 mbar. To this point, the backing pressure of the FT-ICR platform cannot be altered from the manufacturer setting. For membrane protein analysis, the backing pressure on the Q-ToF is typically set around 6.0 mbar [20], which was the backing pressure maintained for the experiments described herein. While lower pressures can be used, the resulting spectra will consist largely of membrane protein-detergent complex signals thus, very heterogenous [20]. Several groups have developed modifications to the source region of the Synapt G1 and G2 instruments to allow for source heating more similar to the FT-ICR [36, 37]. However, given the isolation of these modifications to

specific laboratories, we opted to evaluate the data quality and conditions necessary for optimal protein liberation using the manufacturer provided instrument sources.

Given the two fundamentally different designs of these source regions, a direct comparison of these two voltage settings is challenging. The sampling cone voltage, analogous to Skim1 (FT-ICR), can be manipulated to aid in ion transmission as well as to generate various levels of in source dissociation. However, this voltage is in much closer proximity to the nano-ESI emitter than that of Skiml (FT-ICR). The other voltage setting manipulated on this instrument is the collision energy in the Trap (TrapCE) which is the offset between the exit of the quadrupole and the entrance of the collision cell (Q-ToF TWIG cell; FT-ICR hexapole). The ability to manipulate the energy imparted to these ions at various locations in each instrument allows for thorough investigation of which voltage parameters generate optimal liberation of the membrane proteins from the detergent micelles. Additionally, it allows for determination of which conditions generate intense dissociation of the liberated membrane proteins - leading to subunit stoichiometric information. Exploration of optimal voltage conditions is dependent upon the given pressure settings (backing and trap pressure) of the instrument and could potentially vary upon changes in these values.

FT-ICR native-MS Analysis of the AqpZ Tetramer

Native-MS spectra of detergent solubilized membrane proteins in the absence of collisional activation are typically populated by detergent micelle distribution signal, highly polydisperse in nature (Figures S1-S4, Supporting Information) [38]. As previously mentioned, ion activation is used to increase the protein-to-detergent (P/D; Eq. 1) ratio. Multiple Skim1 voltages were explored (50, 75, 100 and 125 V) which, in the absence of an applied voltage to the collision cell, yielded a polydisperse detergent micelle distribution between m/z 1000-3000 at all voltages (Figures S1-S4, Supporting Information) and produced minimal tetramer protein complex ejection solely at 125 V (Figure S1, Supporting Information). At this voltage, tetramer signal was observed at 5.4% relative intensity to the base peak (Figure S1, Supporting Information). It was instead the combination of the Skim1 and collision cell voltages that generated consistent AqpZ ejection. Increasing the applied CE in the collision cell above 20 V produced varying degrees of AqpZ tetramer ejection from the OG detergent micelle. Higher Skim1 voltages or increase of the CE voltage, (Skim1 75 V with CE 30 V, Skim1 100 V with CE 30-50 V and Skim1 125 V with CE 20-50 V; Figures S1-S4, Supporting Information) generated dissociation of the tetramer into lower MW multimeric species (trimer and monomer; Figures S1 and S2, Supporting Information). The trimeric species, when observed, displayed a maximum of five charge states (z = 8+ to 12+), which at higher CE voltages were more abundant than the tetramer signal (*m/z* 4200-6000). Further increase of the collision cell activation, i.e. up to 50 V, caused further loss of tetramer signal by way of increased dissociation and ultimately led to an inability to observe any signal corresponding to AqpZ. With the exception of several Skim1 and CE voltage combinations, the detergent micelle signal remained relatively intense as compared to protein signal (low P/D) throughout the analysis.

In general, a relatively wide range of Skim1 and collision cell voltages produced some level of intact tetrameric AqpZ signal (Skim1 50 V with CE 30 and 50 V and Skim1 75, 100 and

125 V with CE ranging from 10-40 V; Figures S1-S4, Supporting Information). However, many of these combinations also generated dissociation of the tetramer, while very few settings produced solely intact tetramer (Skim1 50 V with CE 30-40 V, Skim1 75 V with CE 20 and 40V, Skim1 100 V with CE 10-20 V and Skim1 125 V with CE 10 V; Figures S1-S3, Supporting Information). Given the observation of subunit ejection under a variety of source Skim1 and collision cell voltage settings, it is clearly a balance of the applied voltages between these two regions which result in efficient AqpZ liberation, highly consistent with previously described Q-ToF data [34].

Optimal liberation of AqpZ was obtained with the combination of Skim1 50 V and CE activation at 30 V, which were considered optimal conditions due to both the AqpZ tetramer signal intensity as well as the absence of any detectable monomer/subunit ejection. Under these conditions, four major charge states (z = 18+ to 21+) were detected, which correlated with the unmodified tetramer (4 M1) average theoretical MW of 97,074.24 Da (calculated from elemental composition) and a mass accuracy of +89 ppm (Figures 2a and 4S). These mild activation conditions provided a spectrum with an S/N of 111, a P/D of 1.6 and an average charge state of z = 19.6+. Previous native-MS investigation in alternative detergents, such as C_8E_4 and *n*-Nonyl-β-D-glucopyranoside (NG), yielded lower average charge states, as expected for these types of detergents [34, 39]. However, the AqpZ preparation and purification described herein were performed in OG (Supporting Information), thus in order to decrease sample handling prior to MS, OG was also employed during the native-MS analysis.

Examination of the individual tetrameric charge states under optimal protein liberation conditions (Skim1 50 V and CE 30 V) revealed clear superpositioning of five distinct possible proteoforms [40] (Figure 2b). Mass deconvolution of these different proteoforms provided the MW's listed in Figure 2b. Using the apices *m/z* values of the different proteoforms, tetrameric masses that maintained an average of Δ32.23 ± 0.04 Da between each proteoform were obtained. Mass error compared to the theoretical mass of the intact tetramer (with incorporation of the modified monomer) could not be accurately determined for the last four proteoforms (proteoforms B-E in Figure 2) due to the contribution of adjacent proteoforms to the *m/z* ratios of the individual proteoforms. However, this error is expecteed to contribute to the slight shift in the predicted distribution as compared to the experimental observations (Figure 2b, *inset*). At higher CE voltages where lesser multimeric species were observed, their inspection also revealed complementary superpositioning (i.e. trimer consisting of four potential combinations of monomeric species); with the monomeric species showing two distinct signals for each discrete charge state. Mass deconvolution (by MaxEnt 1; [33]) of these two species provided average MW's of 24,270.65 and 24,297.04 Da, designated as M1 and M2, respectively which provided an overall mass difference of Δ26.39 Da. These MW's correlate well to those obtained from the denaturing LC-MS experiments (*vide infra*). The less intense signal to the right of the main AqpZ signal, between *m/z* 4860-4870, differs from the expected AqpZ tetramer MW by an average of Δ31.40 Da. Two oxidation events could potentially account for this signal.

Q-ToF native-MS Analysis of the AqpZ Tetramer

Q-ToF platforms are the most widely utilized analyzers for native-MS of membrane proteins solubilized under a variety of conditions [20, 26, 34], hence AqpZ was also analyzed on an ion mobility Q-ToF. For these experiments, a single sampling cone voltage of 40 V was employed and the Traveling-wave ion guide (TWIG) trap activation voltage was varied, ranging from 10 to 110 V. This produced various levels of protein liberation and subunit ejection from the OG-detergent micelles from 50 to 110 V (Figure S5, Supporting Information). While some previous studies [20, 34] have utilized higher sampling cone voltages (typically 200 V), here variation of this voltage, in both the presence or absence of Trap CE activation, did not provide the same variation of AqpZ tetramer dissociation as observed with variation of the source Skim1 voltage on the FT-ICR. Instead its variation solely affected the observation of detergent micelle signal and the stability of the signal observed. Therefore, a low sampling cone voltage was maintained through the experiments to aid in maintaining mild activation conditions optimal for observation of intact tetramer. Consequently, trapCE variation was the sole voltage parameter investigated for its effect on the obervation of AqpZ tetramer signal.

Optimal AqpZ liberation was observed using a TWIG trap activation voltage of 70 V, as these conditions provided distinguishable tetramer signal with minimal dissociation into trimeric or monomeric substituents. However, even under optimal liberation conditions, the spectrum also maintained an intense detergent micelle distribution in the lower *m/z* range that overpowered the minimal protein tetramer signal (P/D of 0.04), which presented a charge state distribution of $z = 16+$ to 20+ (Figure 3a). Under these conditions, five major charge states ($z = 16+$ to 20+) were detected, which correlated with the calculated tetramer MW, 97074.24 Da (Figure 3b, *inset*). The increased tetramer signal from tandem-MS (Figure 3b) facilitated examination of the discrete tetrameric charge states revealing similar superpositioning to that observed in the FT-ICR data (Figure 2). However, this inspection revealed poorly resolved, yet distinguishable superpositioning of five proteoforms (Figure 3b, *inset*), which was in agreement with the results observed on the FT-ICR. Here the ppm error of the observed proteoforms *m/z* could not be accurately determined as the proteoforms remained poorly resolved, thus contribution from the adjacent proteoforms is highly probable. However in this analysis, the different proteoforms correlated to tetrameric masses that maintained an average of $\Delta 43.39 \pm 21.74$ Da between the apex of each proteoform (Figure 3b, *inset*). Given the minimal resolution between proteoforms, it is important to note that the data presented throughout this work is not post processed in any way (smoothed, background subtracted, etc). Attempts to smooth the data resulted in loss of resolution between these proteoforms depending on the smoothing parameters utilized.

Similar to the observations on the FT-ICR, increasing ion activation (TWIG voltage of 90-110 V) caused a shift in abundance of the tetrameric species to favor the trimeric and monomeric species, which eventually overpowered the signal for the tetrameric complex. Under these conditions, mass deconvolution by MaxEnt1 of the two monomeric species provided MW's of 24,269.48 Da and 24,297.29 Da for M1 and M2, respectively, which provided an overall mass difference of $\Delta 27.81$ Da. Yet while this deconvolution allowed for MW determination of the two monomeric species, it did not explain the physical difference

between the two monomeric species, which was ultimately responsible for the superpositioning observed in the tetramer. This superpositioning was due to various combinations of the two monomeric species (*vide infra*).

Utilization of Tandem-MS to Increase S/N and P/D Ratios through Targeted m/z Experiments

Tandem-MS can be used for interrogation of individual charge states as well as to simplify the analysis of highly polydisperse spectra [22, 41, 42]. It has been previously reported during the investigation of bacteriorhodopsin in OG that employment of tandem-MS on both FT-ICR and Q-ToF instruments did in fact achieve higher P/D and S/N ratios for the protein [22]. This was accomplished through selection of several *m/z* ratios both slightly higher and in the middle of the expected *m/z* range of the charge state distribution for the protein. Here, tandem-MS was employed in this fashion to determine if similar increases in S/N and P/D ratios would be observed for a larger multimeric membrane protein complex.

In full-MS mode, FT-ICR analysis generally provided low P/D ratios at the various Skim1 and CE voltages investigated than the Q-ToF. Under optimal ejection conditions, tandem-MS was investigated by selecting *m/z* 5900, 5500 and 5000, while maintaining the acquisition *m/z* range of 153-10,000 to allow for observation of potential tetramer dissociation. However, none of the precursor *m/z* selections investigated provided recognizable protein signal and in fact, in all cases provided only unstable detergent signal (data not shown). A similar strategy was employed on the Q-ToF while maintaining its respective optimal ejection conditions and acquisition *m/z* range of 500-10,000. The quadrupole selection window on this platform is set using LM and HM resolution slider values. For these experiments values of 4 and 10, were used for the LM and HM values respectively, which equate to a transmission window of 24 *m/z* at FWHM (based on native MS/MS quad selection of BSA at *m/z* 4457.42). First, the *m/z* ratio 6500 (slightly above the tetramer charge state distribution) was selected which increased the P/D roughly 100-fold (P/D = 2.8) while maintaining the same charge distribution as observed in full-MS mode (Figures 3 and 4a). Interestingly, the *m/z* targeted during tandem-MS had an effect not only on the observed tetramer charge state distribution, but also on the observation of AqpZ monomer signal (Figure 4). Decreasing precursor selection from *m/z* 6500 to *m/z* 5500 shifted the average tetramer charge state from $z = 18.1+$to $z = 20.1+$, and resulted in the observation of intense monomer signal (charge states $z = 7+$ to 11+). This observation could be explained by the selection of higher tetrameric charge states as the *m/z* ratio selected is decreased. These higher charge states require less activation energy to undergo asymmetric subunit dissociation than lower charge states, thus more dissociation into its respective monomer and trimeric constituents was observed [42, 43].

Some tandem-MS studies of soluble proteins have demonstrated that the energies necessary to dissociate higher order complexes is dependent upon the charge state isolated during the tandem-MS experiment [42, 44]. For example, it was observed that if the dodecameric SP-1 charge state isolated was higher than $z = 24+$ it dissociated mainly through ejection of higher oligomers, while if lower than $z = 24+$, the complex dissociated mainly through ejection of monomers. Thus depending on the charge state isolated, the complex may dissociate via

several different mechanisms. Here, given the shift in average tetrameric charge state observed we can deduce similar charge dependent effects on dissociation. However, it is unclear why tandem-MS showed no effect in generating high S/N mass spectra for AqpZ tetramer in OG using the FT-ICR platform, whereas it is an effective strategy using the Q-ToF instrument. The roles of OG micelle size and how the FT-ICR instrument effectively removed detergent molecules from the membrane protein, as was reported for the Q-ToF system [39] will be investigated in the future.

Denaturing LC-MS for Monomer Accurate Mass and Identification of the Δ27.14 Da Mass Addition by Proteolytic Digestion Followed by LC-MS/MS

Denaturing LC-MS was employed to obtain accurate mass measurements for the two monomeric species identified as a consequence of CID activation of the AqpZ tetramer. For this experiment, AqpZ in 200 mM ammonium acetate and 1.1% (w/v) OG was diluted to 0.5 μg/μL and 0.125 μg AqpZ was injected on the C3 column and analyzed using a 15 minute gradient (*Experimental*). The resulting spectrum (Figure S6, Supporting Information) revealed two monomeric species with MW's of 24,267.76 Da and 24,294.90 Da for M1 and M2, respectively. The M1 species corresponded to the monomeric AqpZ sequence minus the two C-terminus amino acid residues glycine and serine. The M2 MW corresponded to the M1 sequence with a 27.14 Da mass addition. Given the various potential sources of the mass addition, such as single amino acid substitutions of serine with asparagine (+27.01 Da), lysine with arginine (+28.01 Da) or formylation (+27.99 Da), further investigation by enzymatic digestion was performed.

The solution conditions for each of the three enzymatic digestions can be found in the *Experimental* section. The level of sequence coverage from combining the spectral information for all three digestions equated to only 55% coverage, with the Lys-C digestion providing the least coverage (2.94%) to chymotrypsin, which predictably provided the most (54.6%) (Figure 5a). Yet while the level of sequence coverage was less than ideal, it was observed that the N-terminal peptides from both the trypsin and the chymotrypsin digests presented two very distinct peaks that differed by over 10 minutes in retention time (Figure S7, Supporting Information). Further investigation of the two chromatographic peaks from the tryptic digest revealed that the corresponding peptides that eluted (deconvoluted monoisotopic masses: un-modified = 452.2224 Da and modified = 480.2182 Da) differed in mass by Δ27.9958 Da, with the modified peptide maintaining the longer retention time. The fact that a 27.9958 Da mass addition was observed in the N-terminal peptides from both the tryptic and chymotryptic digests meant that the source of the mass addition could be isolated to the three N-terminal amino acid residues MFR. Given the three amino acids present in the tryptic digest N-terminal peptide and taking into account the potential modification sources of the addition, it was hypothesized that N-terminal methionine formylation (fMet) was in fact the modification present as there was only 5 ppm error between the observed mass and the theoretical mass of a formylated peptide. This hypothesis was confirmed by targeted CID of the modified and unmodified N-terminal ***MFR*** peptide from the tryptic digest (Figures 5b and 5c) which yielded unique b2, b3-NH_3 and y3 ions, contingent upon the specific peptide fragmented.

Leveraging the Advantages of the Individual FT-ICR and Q-ToF Platforms

There has long been discussion in the MS community regarding the energetic differences between various MS platforms. It would be amiss not to discuss the distinct differences of the FT-ICR and Q-ToF platforms explored here that give rise to the unique experimental conditions for optimal protein liberation from the detergent micelles. The source voltages must remain at a minimum to allow for efficient transmission of the intact protein-micelle complex with minimal dissociation. Thus, it is the downstream application of collision energy (Q-ToF TWIG cell; FT-ICR hexapole) that disrupts the protein-micelle complex to liberate the protein. The intrinsically different source designs prevent an accurate comparison of the exact conditions. However, it must be considered that the ions transit through a heated ion transfer capillary in the FT-ICR source. It could be hypothesized that the thermal energy imparted into the protein-micelle complex is sufficient to increase its internal energy (i.e. rotational, vibration and translational) such that less activation energy is required for protein ejection in either the Skim1 or hexapole collision cell region. It is therefore important to note the distinct effect of increasing the Skim1 voltage on the FT-ICR which, when the applied collision cell energy remained constant (30 V), generated spectra with varying amounts of tetramer dissociation. Thus implying that some level of dissociation occurs in the source regime due to ion neutral collisions with residual gas prior to the collision cell. However, variation of the sampling cone voltage on the Q-ToF had virtually no effect on the amount of tetramer observed, regardless of the applied trapCE. These observations support the hypothesis of more efficient desolvation within the longer heated capillary of the FT-ICR, which allowed for the observation of tetramer at higher Skim1 voltages (100 and 125 V) even in the presence of minimal collision energy (10 and 20 V; Supporting Information Figures IS and 2S).

Resolution limitations in native-MS are indeed of concern when analyzing large protein systems [45] which could contain various levels of small modifications and/or bound ligand. We feel it is important to note that the FT-ICR enabled clear distinction of proteoform masses because there will be cases where the make-up of these multimeric membrane protein complexes could have an impact on their function and thus their overall biological significance. As well, the increase in resolution provided by the FT-ICR would enable increased confidence in the determination and assignment of small-molecule binding to membrane proteins and their complexes. As pointed out previously, this class of molecules represents a key area of interest for the pharmaceutical industry. Thus making the identification of drug binding/incorporation into these proteins a key sub-area of importance. Additionally, numerous other low MW modifications may be of potential interest during the characterization of other membrane protein complexes, such as non-covalently bound lipids, bound small molecule drug candidates and post translational modifications [7, 23, 46, 47]. As these proteins naturally exist within a lipid membrane, the ability to observe and identify bound lipid species could provide key insights into the natural membrane environment of a protein target [2, 34].

Conclusions

This work demonstrates, to our knowledge, the first analysis of a multimeric membrane protein complex by FT-ICR. Direct comparison of the spectral quality achieved under optimal protein ejection conditions on the FT-ICR to that obtained on the Q-ToF provides strong support for the continued use of FT-ICR-MS for membrane protein analysis. While proteoform resolution was readily observed in the FT-ICR data, essentially no proteoform resolution was observed on the Q-ToF without quadurpole selection. Employment of quadrupole selection was also necessary on the Q-ToF platform to achieve comparable S/N and P/D ratios (S/N of 111, P/D of 1.6 and S/N of 85, P/D 2.8 for the FT-ICR and Q-ToF, respectively), while minimal collision energy was needed on the FT-ICR.

Resolution and *m/z* separation power are important characteristics to consider for any sample, but are of particular importance when analyzing complex samples with potential low MW modifications as it facilitates their observation. As well, it can provide insight as to how those modifications may affect protein subunit integration into a membrane protein complex [1]. Closer investigation of the tetramer complex signal here revealed superpositioning, which was ultimately attributed to multiple combinations of both an N-terminally formylated and a non-formylated monomer through proteolytic digests and targeted LC-MS/MS. While not the most biologically relevant modification, the presence of fMet did indeed contribute to the complexity of the data analysis. However, the ability to better separate and more clearly assign the proteoform superpositioning here provides an optimistic outlook that, with the superior *m/z* separation power of the FT-ICR, the potential presence of low MW modifications could be determined. Given the low biological significance of the N-terminal formylation present, it is inappropriate to draw inference into the biological relevance of the various compositions based on their corresponding intensities. However, this characterization provides an important piece of information regarding the protein composition prior to any sample handling that might alter the protein structure post cell-expression and prior to native-MS investigation. Previous studies regarding N-terminal methionine excision from *E. coli* expressed proteins have shown that excision is heavily dictated by the identity of the penultimate amino acid residue [48]. In those experiments it was observed that when phenylalanine was present in the penultimate position, excision of the methionine was not observed [48], which is in accordance with the observations detailed in this analysis. It can be speculated that this is a contributing factor to why the N-terminal fMet, a common modification in *E. coli* expressed proteins [48, 49] is observed here.

To the best of our knowledge, the observation of this low MW modification on the AqpZ tetramer has not been previously reported. Given its small mass, this formylation and other similar modifications could easily be overlooked depending upon the instrumental parameters utilized and/or the post-acquisition data processing (such as smoothing) procedures employed. Careful attention to the instrumental conditions employed on lower resolution platforms as well as data processing settings will be absolutely essential to ensure that subtle details within the protein charge state distribution are not overlooked. It should be reiterated that the data presented from both platforms was not post processed in any way (i.e. smoothing, background subtraction, etc). Smoothing of the FT-ICR data still allowed for the proteoform superpositioning to be observed while the ability to retain proteoform resolution

in the Q-ToF data was extremely dependent on the smoothing method and parameters applied. The ability to post process data without loss of resolution of low level modifications, provides strong support for the use of the FT-ICR platform for multimeric membrane protein complex analysis, at least in combination with a Q-ToF platform when possible. The range of applicable collision voltage prior to complete complex dissociation was narrower on the FT-ICR platform than the Q-ToF; which suggests that for structural studies, the Q-ToF platform would provide superior range for probing structural stability (Figures S1-S3, Supporting Information). However, it is clearly demonstrated that the superior resolution of the FT-ICR makes it a strong candidate for the analysis of membrane proteins that may contain small MW modifications. In any case, we predict that due to the increased S/N and P/D levels, higher level of protein desolvation and increased resolution provided by the FT-ICR that it will continue to gain popularity as an important platform for the characterization of multimeric protein complexes.

Supplementary Material

Refer to Web version on PubMed Central for supplementary material.

Acknowledgments

Support from the US National Institutes of Health (R01GM103479 and S10RR028893) and the US Department of Energy (UCLA/DOE Institute for Genomics and Proteomics; DE-FC03-02ER63421) to J.A.L. is acknowledged. The postdoctoral program at Amgen, Inc is acknowledged for its support of this project.

References

1. Almen MS, Nordstrom Karl JV, Fredriksson Robert, Schioth Helgi B. Mapping the human membrane proteome: a majority of the human membrane proteins can be classified according to function and evolutionary origin. BioMed Central Biology. 2009; 7(50)
2. Barrera NP, Min Z, Robinson Carol V. The role of lipids in defining membrane protein interactions: insights from mass spectrometry. Trends in Cell Biology. 2013; 23(1):1–8. [PubMed: 22980035]
3. Hopkins, ALa, G, Colin R. The druggable genome. Native Reviews Drug Discovery. 2002; 1:727–730.
4. Arinaminpathy Y, K Ekta, Engelman Donald M, Gerstein Mark B. Computational analysis of membrane proteins: the largest class of drug targets. Drug Discovery Today. 2009; 14(23-24):1130–1135. [PubMed: 19733256]
5. Carpenter EP, Konstantinos B, Cameron Alexander D, Iwata So. Overcoming the challenges of membrane protein crystallogrpahy. Current Opinion in Structural Biology. 2008; 18(5):581–586. [PubMed: 18674618]
6. Bill, Roslyn M., Henderson, PJFI., Kunji, So, Edmund, RS., Michel, Hartmut, Neutze, Richard, Newstead, Simon, Poolman, Bert, Tate, Christopher G., Vogel, Horst. Overcoming barriers to membrane protein structure determination. Nature Biotechnology. 2011; 29(4):335–340.
7. Landreh, MaR, Carol, V. A new window into the molecular physiology of membrane proteins. The Journal of Physiology. 2015:355–362. [PubMed: 25630257]
8. Stansfeld PJG, Joseph E, Caffrey Martin, Carpenter Elisabeth P, Parker Joanne L, Newstead Simon, Sansom Mark SP. MemProtMD: Automated Insertion of Membrane Protein Structures into Explicit Lipid Membranes. Structure. 2015; 23(7):1350–1361. [PubMed: 26073602]
9. Barrera, NPaR, Carol, V. Advances in the Mass Spectrometry of Membrane Proteins: From Individual Proteins to Intact Complexes. The Annual Review of Biochemistry. 2011:247–271.

10. le Coutre JW, Julian P, Gross Adrian, Turk Eric, Wright Ernest M, Kaback H Ronald, Faull Kym F. Proteomics on Full-Length Membrane Proteins Using Mass Spectrometry. Biochemistry. 2000; 39:4237–4242. [PubMed: 10757971]
11. Savage DFE, Pascal F, Robles-Colmenares Yaneth, O′Connell Joseph D III, Stroud Robert M. Architecture and Selectivity in Aquaporins 2.5: A X-Ray Structure of Aquaporin Z. PLOS Biology. 2003; 1(3):334–340.
12. Wang SC, Argyris P, Di Bartolo Natalie, Bavro Vassiliy N, Tucker Stephen J, Booth Paula J, Barrera Nelson P, Robinson Carol V. Ion Mobility Mass Spectrometry of Two Tetrameric Membrane Protein Complexes Reveals Compact Structures and Differences in Stability and Packing. Journal of the American Chemical Society. 2010; 132:15468–15470. [PubMed: 20949939]
13. Chang, YCa, B, James U. Measuring membrane protein stability under native conditions. Proceedings of the National Academy of Sciences. 2014; 111(1):219–224.
14. Fisette O, Christopher P, Barnes Ryan, Isas J Mario, Langen Ralf, Heyden Matthias, Han Songi, Schafer Lars V. Hydration Dynamics of a Peripheral Membrane Protein. Journal of the American Chemical Society. 2016; 138:11526–11535. [PubMed: 27548572]
15. Marcoux, Ja, R, Carol V. Twenty Years of Gas Phase Structural Biology. Structure. 2013; 21(9): 1541–1550. [PubMed: 24010713]
16. Whitelegge JPG, Cameron B, Faull Kym F. Electrospray-ionization mass spectrometry of intact intrinsic membrane proteins. Protein Science. 1998; 7:1423–1430. [PubMed: 9655347]
17. Barrera NP, DB N, Booth PJ, Robinson Carol V. Micelles protect membrane complexes from solution to vacuum. Science. 2008; 321(5886):243–246. [PubMed: 18556516]
18. Zhou M, M Nina, Barrera Nelson P, Politis Argyris, Isaacson Shoshanna C, Matak-Vinkovic Dijana, Murata Takeshi, Bernal Ricardo A, Stock Daniela, Robinson Carol V. Mass Spectrometry of Intact V-Type ATPases Reveals Bound Lipids and the Effects of Nucleotide Binding. Science. 2011; 334(6054):380–385. [PubMed: 22021858]
19. Housden NGH, Jonathan TS, Lukoyanova Natalya, Rodrigues-Larrea David, Wojdyla Justyna A, Klein Alexander, Kaminska Renata, Bayley Hagan, Saibil Helen R, Robinson Carol V, Kleanthous Colin. Intrinsically Disordered Protein Threads Through the Bacterial Outer-Membrane Porin OmpF. Science. 2013; 340(6140):1570–1574. [PubMed: 23812713]
20. Laganowsky A, Eamonn R, Hopper Jonathan TS, Robinson Carol V. Mass Spectrometry of intact membrane protein complexes. Nature Protocols. 2013; 8(4):639–651. [PubMed: 23471109]
21. Mikhailov VA, L Idlir, Mize Todd H, Bush Matthew F, Benesch Justin LP, Robinson Carol V. Infrared Laser Activation of Soluble and Membrane Protein Assemblies in the Gas Phase. Analytical Chemistry. 2016; 88(14):7060–7067. [PubMed: 27328020]
22. Campuzano IDG, Huilin L, Bagal Dhanashri, Lippens Jennifer L, Svitel Juraj, Kurzeja Robert JM, Xu Han, Schnier Paul D, Loo Jospeh A. Native MS Analysis of Bacteriorhodopsin and an Empty Nanodisc by Orthogonal Acceleration Time-of-Flight, Orbitrap, and Ion Cyclotron Resonance. Analytical Chemistry. 2016
23. Gault JD, Joseph AC, Liko Idlir, Hopper Jonathan TS, Gupta Kallol, Housden Nicholas G, Struwe Weston B, Marty Michael T, Mize Todd, Bechara Cherine, Zhu Ya, Wu Beili, Kleanthous Colin, Belov Mikhail, Damoc Eugen, Makarov Alexander, Robinson Carol V. High-resolution mass spectrometry of small molecules bound to membrane proteins. Nature Methods. 2016
24. Hopper JTS, Yvonne Y Ting Chen, Li Dianfun, Raymond Alison, Bostock Mark, Liko Idlir, Mikhailov Victor, Laganowsky Arthur, Benesch Justin LP, Caffrey Martin, Nietilispach Daniel, Robinson Carol V. Detergent-free mass spectrometry of membrane protein complexes. Nature Methods. 2013; 10:1206–1208. [PubMed: 24122040]
25. Calabrese ANW, Thomas G, Henderson Peter JF, Radford Sheena E, Ashcroft Alison E. Amphipols Outperform Dodecylmaltoside Micelles in Stabilizing Membrane Protein Structure in the Gas Phase. Analytical Chemistry. 2015; 87(2):1118–1126. [PubMed: 25495802]
26. Marty MT, Kin Kuan H, Robinson Carol V. Interfacing Membrane Mimetics with Mass Spectrometry. Journal of the American Chemical Society. 2016; 49(11):2459–2467.
27. Bayburt THG, Yelena V, Sligar Stephen G. Self-Assembly of Discoidal Phospholipid Bilayer nanoparticles with Membrane Scaffold Proteins. Nano Letters. 2002; 2(8):853–856.

28. Marty MT, Z H, Cui W, Blankenship RE, Gross ML, Sligar SG. Native Mass Spectrometry Charaterizes Intact Nanodisc Lipoprotein Complexes. Analytical Chemistry. 2012; 84(21):8957–8960. [PubMed: 23061736]
29. Dorr JMK, Martijn C, Schafer Marre, Prokofyev Alexander V, Scheidelaar Stefan, van der Cruijsen Elwin AW, Dafforn Timothy R, Baldus Marc, Killian J Antoinette. Detergent-free isolation, characterization, and functional reconstitution of a tetrameric K^+ channel: The power of native nanodiscs. Proceedings of the National Academy of Sciences. 2014; 111(52):18607–19612.
30. van de Waterbeemd M, Snijder Joost, Tsvetkova Irina B, Dragnea Bordan G, Cornelissen Jeroen J, Heck Albert JR. Examining the Heterogenous Genome Content of Multipartite Viruses BMV and CCMV by Native Mass Spectrometry. Journal of The American Society for Mass Spectrometry. 2016; 27(6):1000–1009. [PubMed: 26926442]
31. Lange O, D Eugne, Wieghaus Andreas, Makarov Alexander. Enhanced Fourier transform for Orbitrap mass spectrometry. International Journal of Mass Spectrometry. 2014; 369:338–344.
32. Makarov A, D Eduard, Lange Oliver, Horning Stevan. Dynamic Range of Mass Accuracy in LTQ Orbitrap Hybrid Mass Spectrometer. Journal of The American Society for Mass Spectrometry. 2006; 17(7):977–982. [PubMed: 16750636]
33. Ferrige AG, S MJ, Green BN, Jarvis SA, Skilling J, Staunton J. Disentangling electrospray spectra with maximum entropy. Rapid Communications in Mass Spectrometry. 1992; 6(11):707–711.
34. Laganowsky A, R Eamonn, Allison Timothy M, Ulmschneider Martin B, Degiacomi Matteo T, Baldwin Andrew J, Robinson Carol V. Membrane proteins bind lipids selectively to modulate their structure and function. Nature. 2014; 510(7503):172–175. [PubMed: 24899312]
35. Liu Y, C Xiao, Liu Wen, Laganowsky Arthur. Characterization of Membrane Protein-Lipid Interactions by Mass Spectrometry Ion Mobility Mass Spectrometry. Journal of The American Society for Mass Spectrometry. 2016
36. Cong X, Lang L, Liu Wen, Liang Xiaowen, Russell David H, Lagonowsky Arthur. Determining Membrane Protein-Lipid Binding Thermodynamics Using Native Mass Spectrometry. Journal of the American Chemical Society. 2016; 138:4346–4349. [PubMed: 27015007]
37. Lippens JL, M JB, McIntyre William, Redick Bill, Fabris D. A simple heated-capillary modification improves the analysis of non-covalent complexes by Z-spray electrospray ionization. Rapid Commun Mass Spectrom. 2016; 30:773–783. [PubMed: 26864529]
38. Borysik AJH, Dominic J, Robinson Carol V. Detergent Release Prolongs the Lifetime of Native-like Membrane Protein Conformations in the Gas-Phase. Journal of the American Chemical Society. 2013; 135:6078–6083. [PubMed: 23521660]
39. Reading E, L Idlir, Allison Timothy M, Benesch Justin LP, Laganowsky Arthur, Robinson Carol V. The Role of the Detergent Micelle in Preserving the Structure of Membrane Proteins in the Gas Phase. Angewandte Chemie. 2015; 54(15):4577–4581. [PubMed: 25693501]
40. Smith, LMaK, Neil, L. Proteoform: a single term describing protein complexity. Nature Methods. 2013; 10:186–187. [PubMed: 23443629]
41. Benesch JL, PA J Andrew, Ruotolo Brandon T, Sobott Frank, Robinson Carol V. Tandem Mass Spectrometry Reveals the Quartenary Organization of Macromolecular Assemblies. Chemistry and Biology. 2006; 13(6):597–605. [PubMed: 16793517]
42. Benesch JLPR, Brandon T, Sobott Frank, Wildgoose Jason, Gilbert Anthony, Bateman Robert, Robinson Carol V. Quadrupole-Time-of-Flight Mass Spectrometer Modified for Higher-Energy Dissociation Reduces Protein Assemblies to Peptide Fragments. Analytical Chemistry. 2009; 81(3):1270–1274. [PubMed: 19105602]
43. Pagel K, H Suk Joon, Ruotolo Brandon T, Robinson Carol V. Alternative Dissociation Pathways Identified in Charge-Reduced Protein Complex Ions. Analytical Chemistry. 2010; 82(12):5363–5372. [PubMed: 20481443]
44. Erba EBR, Brandon T, Barsky Daniel, Robinson Carol V. Ion Mobility-Mass Spectrometry Reveals the Influence of Subunit Packing and Charge on the Dissociation of Multiprotein Complexes. Analytical Chemistry. 2010; 82(23):9702–9710. [PubMed: 21053918]
45. Lossl P, S Joost, Heck Albert JR. Boundaries of Mass Resolution in Native Mass Spectrometry. Journal of The American Society for Mass Spectrometry. 2014; 25(6):906–917. [PubMed: 24700121]

46. Katada, Ta, U, Michio. Direct modification of the membrane adenylate cyclase system by islet-activating protein due to ADP-ribosylation of a membrane protein. Proceedings of the National Academy of Sciences. 1982; 79:3129–3133.

47. Yen HYH, Jonathan TS, Liko Idlir, Allison Timothy M, Zhu Ya, Wang Dejian, Stegmann Monika, Mohammed Shabez, Wu Beili, Robinson Carol V. Ligand Binding to a G protein-coupled receptor captured in a mass spectrometer. Science Advances. 2017; 3(6)

48. Hirel PH, S Jean Marie, Dessen Philippe, Fayat Guy, Blanquet Sylvain. Extent of N-terminal methionine excision from Escherichia coli proteins is governed by the side-chain length of the penultimate amino acid. Proceedings of the National Academy of Sciences. 1989; 86:8247–8251.

49. Spector SF, Julia M, Tidor Bruce, Baker Tania A, Sauer Robert T. Expresstion of N-formylated proteins in Escherichia Coli. Protein Expression and Purification. 2003; 32:317–322. [PubMed: 14965779]

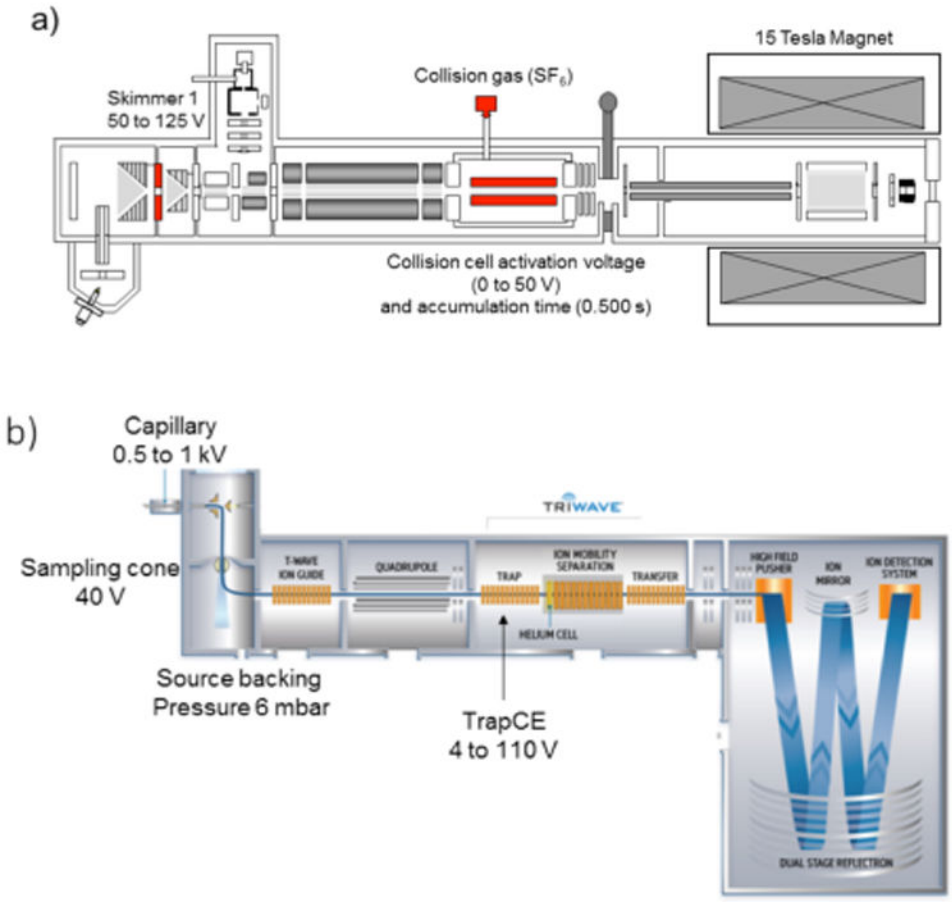

Figure 1.

Instrument schematics of both a) the 15-Tesla FT-ICR, highlighting the Skimmer 1 and collision cell regions; and b) the Synapt G2 quadrupole ion mobility ToF, highlighting the Sampling cone and TrapCE voltage regions. Voltage values shown reflect those used in the experiments detailed in this manuscript.

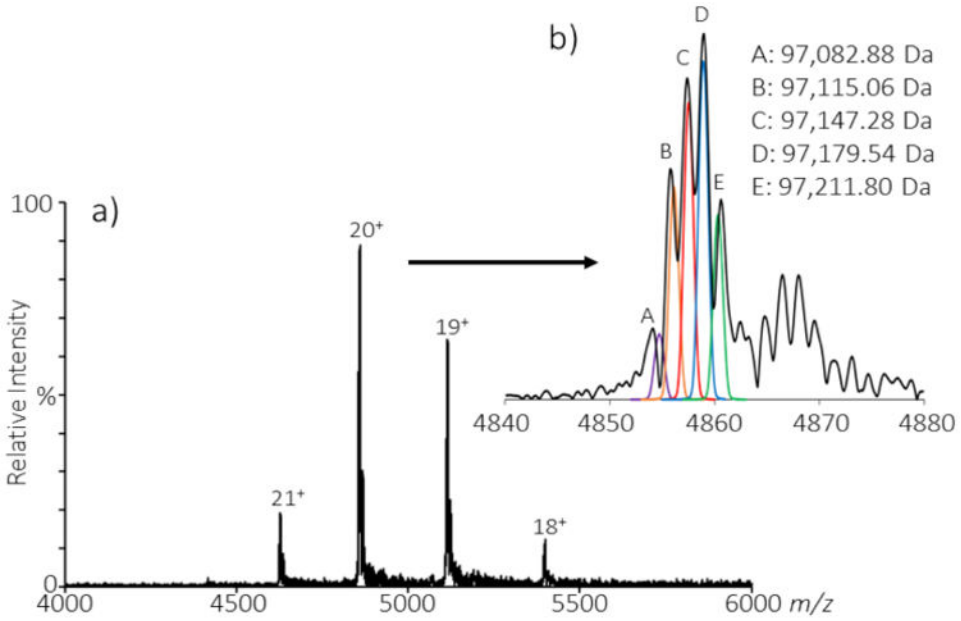

Figure 2.

AqpZ native mass spectra acquired on the FT-ICR; a) mass spectrum collected at Skim 1 50 V and collision cell at 30 V, *m/z* 4000-6000 showing the tetrameric complex and; b) Zoom in of the $z = 20+$ charge state displaying the superpositioning of proteoforms corresponding tetrameric MW's. These proteoforms represent N-terminal formylation, *vide infra* and were observed for each tetrameric charge state. The colored distribution corresponds to the predicted observance of the various proteoforms normalized to the intensity of the tetrameric distribution observed. The proteoforms are colored according to the following monomeric species combinations, for which theoretical MW's, calculated from elemental composition, are provided for each: 4 M1: 97,074.24 Da (purple); 3 M1/2 M2: 97,102.25 Da (orange); 2 M1/2 M2: 91,730.26 Da (red); 1 M1/3 M2: 97,158.27 Da (blue) and 4 M2: 97,186.28 Da (green). MW values provided for species A-E in the inset were calculated from the individual apices *m/z* values. The predicted proteoform distribution *m/z* values as compared to the apices of the experimental peaks differ by 0.58, 0.38, 0.16, -0.06 and -0.27, respectively. The peak distribution to the right of the AqpZ signal differs from the expected AqpZ tetrameric MW by an average of 31.40 Da. This mass difference could potentially be explained by two oxidation events.

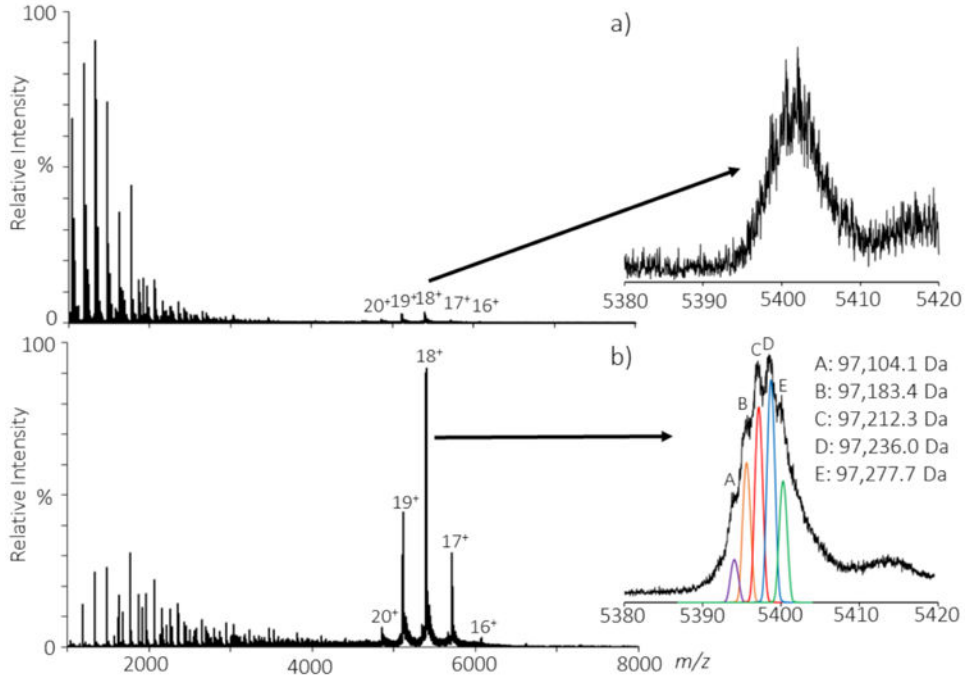

Figure 3.

Native-MS Q-ToF data of AqpZ. a) Full-MS data showing low P/D with intense detergent signal from *m/z* 1000-2500. Sampling cone and TWIG trap voltage at 40 V and 70 V, respectively. Inset shows the lack of proteoform resolution observed for the individual charge states and highlights that in full-MS mode the tetramer is still slightly adducted; and b) Tandem-MS data with the quadrupole selection at *m/z* 6500 showing improved P/D. Acquisition conditions were otherwise kept consistent for both spectra. Inset shows the superpositioning for the 18+ charge state of different proteoforms for this tetrameric protein complex with the corresponding tetrameric MW's. The colored distribution corresponds to the predicted observance of the various proteoforms normalized to the intensity of the tetrameric distribution observed on the FT-ICR. The proteoforms are colored according to the following monomeric species combinations: 4 M1 (purple); 3 M1/1 M2 (orange); 2 M1/2 M2 (red); 1 M1/3 M2 (blue) and 4 M2 (green). The Q-ToF data presented in this figure, and throughout the manuscript, has not been smoothed or post processed. This lack of post processing clearly demonstrates that tandem-MS followed by collisional activation improves the proteoform resolution as compared to full-MS followed by activation for this large multimeric complex.

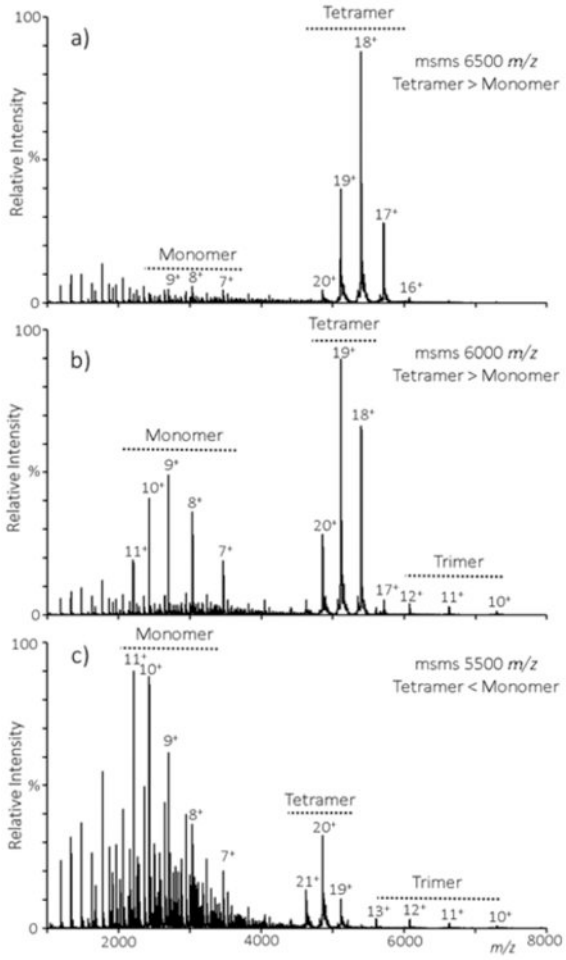

Figure 4.

Use of quadrupole selection to improve the P/D ratio of AqpZ on the ion mobility Q-ToF. a) *m/z* 6500 shows intense tetramer signal with minimal observable monomer species; b) *m/z* 6000 maintains a closer equilibrium of tetramer and monomer species with minimal trimer species observed and; c) *m/z* 5500 is predominantly monomer signal with low intensity tetramer signal as well as trimer signal.

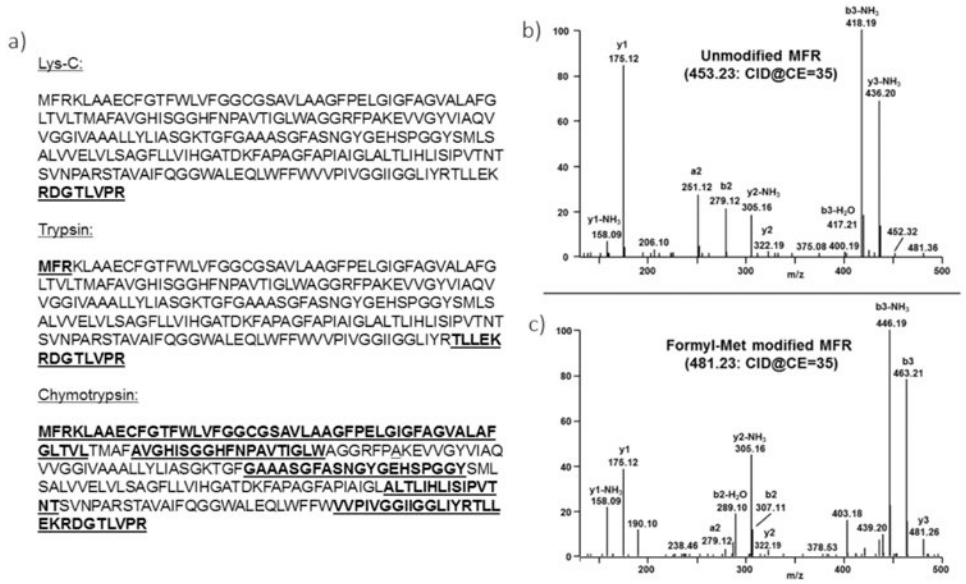

Figure 5.

Characterization of the modification to the monomeric species: a) Sequence coverage of AqpZ from the Lys-C, trypsin and chymotrypsin digestions. Positive sequence identification is underlined; b) Targeted CID spectra of both the unmodified N-terminal peptide from the tryptic digest and; (c) Targeted CID spectra of both the modified N-terminal peptide from the tryptic digest. Both spectra were obtained on the OrbiTrap Velos.